Most microRNAs in the single-cell alga Chlamydomonas reinhardtii are produced by Dicer 2 like 3-mediated cleavage of introns and untranslated regions of coding RNAs

Most microRNAs in the single-cell alga *Chlamydomonas reinhardtii* are produced by Dicer like 3-mediated cleavage of introns and untranslated regions of coding RNAs.

Adrian A. Valli, Bruno A.C.M. Santos, Silvia Hnatova, Andrew R. Bassett[1], Attila Molnar[2], Betty Y. Chung and David C. Baulcombe[3]

Department of Plant Sciences, University of Cambridge, Cambridge, United Kingdom

Current addresses:

[1] Sir William Dunn School of Pathology, University of Oxford, United Kingdom

[2] Institute of Molecular Plant Sciences, University of Edinburgh, Edinburgh, United Kingdom

[3]Correspondence to: dcb40@cam.ac.uk

Running title: Coding RNAs are miRNA precursors in *C. reinhardtii*

Keywords: Algae, RNA silencing, microRNAs, Dicer.

ABSTRACT

We describe here a forward genetic screen to investigate the biogenesis, mode of action and biological function of miRNA-mediated RNA silencing in the model algal species *Chlamydomonas reinhardtii*. Amongst the mutants from this screen there were three at *Dicer-like 3* that failed to produce both miRNAs and siRNAs and others affecting diverse post-biogenesis stages of miRNA-mediated silencing. The DCL3-dependent siRNAs fell into several classes including transposon- and repeat-derived siRNAs as in higher plants. The DCL3-dependent miRNAs differ from those of higher plants, however, in that many of them are derived from mRNAs or from the introns of pre-mRNAs. Transcriptome analysis of the wild type and *dcl3* mutant strains revealed a further difference from higher plants in that the sRNAs are rarely negative switches of mRNA accumulation. The few transcripts that were more abundant in *dcl3* mutant strains than in wild type cells were not due to sRNA-targeted RNA degradation but to direct DCL3 cleavage of miRNA and siRNA precursor structures embedded in the untranslated (and translated) regions of the mRNAs. This analysis reveals that the miRNA pathway in *C. reinhardtii* differs from that of higher plants and resembles that of animals in terms of miRNA precursor structure, domain structure of DCL and in that the target mRNAs persist in the presence of miRNAs. Altogether, our findings inform the understanding of the evolution and function of miRNA-mediated RNA silencing in eukaryotes.

INTRODUCTION

RNA silencing in eukaryotes controls gene expression and protects against viruses and transposons (Baulcombe 2004). Small (s)RNAs of 20-to-31 nucleotides form RNA-induced silencing complexes (RISC) with proteins of the Piwi/Argonaute family (AGO) and they guide these effector proteins to their targets by complementary base pairing (Meister 2013). AGO proteins achieve posttranscriptional gene silencing (PTGS) by target transcript degradation or translational repression, and they promote transcriptional gene silencing (TGS) via chromatin/DNA modifications (Brodersen and Voinnet 2009; Castel and Martienssen 2013).

Corresponding to these various RNA silencing pathways there are multiple types of sRNA that differ in their biogenesis mechanism or in their associated AGO isoform. These sRNAs include small interfering (si)RNAs, micro(mi)RNAs and piwi-interacting (pi)RNAs (Ghildiyal and Zamore 2009). The siRNAs and miRNAs are produced by the action of RNase III Dicer (Dcr) or Dicer-like (DCL) proteins on fully- or near-complementary double-stranded (ds)RNA molecules (Carthew and Sontheimer 2009) whereas piRNAs are Dcr-independent and they have single stranded RNA precursors (Iwasaki et al. 2015).

The miRNAs of plants and animals are similar: they are 20-to-24 nt and derived from precursor RNAs with stem-loop structures (Brodersen and Voinnet 2009). However, there are also clear differences. The biogenesis of animal miRNAs, for example, involves processing of a primary miRNA transcript by various nucleases, including the microprocessor Drosha/DGCR8 to form a miRNA precursor that is then cleaved by Dcr in the cytoplasm (Bartel 2009). Plant miRNAs in contrast are processed in a nuclear DCL-mediated mechanism (Brodersen and Voinnet 2009). There are other differences based on the composition of the AGO complex, requirement for sequence complementarity between the miRNA and its target and the ways that translation is suppressed. These differences prompted the speculation that miRNAs have evolved independently in plant and animal lineages (Axtell et al. 2011).

Most information about miRNAs is from multi-cellular organisms, although they are also present in unicellular organisms including the green alga *Chlamydomonas reinhardtii* (Molnár et al. 2007;

Zhao et al. 2007), protozoans *Giardia lamblia* (Saraiya and Wang 2008), *Trichomonas vaginalis* (Chen et al. 2009), *Pentatrichomonas hominis* (Huang et al. 2012), *Symbiodinium microadriaticum* (Baumgarten et al. 2013), *Entamoeba histolytica* (Mar-Aguilar et al. 2013), *Trypanosoma brucei* (Mallick et al. 2008) and *Toxoplasma gondii* (Braun et al. 2010). These organisms are descended from ancient ancestors of multicellular organisms and they provide an opportunity to test hypotheses about the origin of miRNA pathways.

Here we focus on *C. reinhardtii*, which is from a lineage that diverged from the ancestor of land plants over one billion years ago (Yoon et al. 2004). It has a complex RNA silencing machinery with three DCLs (DCL1-3) and three AGOs (AGO1-3) (Merchant et al. 2007; Casas-Mollano et al. 2008). These proteins are not encoded by orthologues of genes in higher plants although it is well established that *C. reinhardtii* sRNAs, including miRNAs, are like those of higher plants in that they direct cleavage of their mRNA targets (Molnár et al. 2007; Zhao et al. 2007). To investigate the biogenesis, mode of action and biological function of miRNAs in *C. reinhardtii* we have carried out a forward genetic screen in this genetically tractable organism.

RESULTS

Isolation of RNA silencing mutants in *C. reinhardtii*

To characterise mechanisms and biological function of RNA silencing in *C. reinhardtii* we used a reporter system in which a nitrate-inducible artificial (a)miRNA was targeted to the 5' region of the phytoene synthase (PSY) mRNA (ni-amiRNA-PSY, Figure 1A, Figure S1). The amiRNA was readily detectable by northern blotting in cells using nitrate rather than ammonium as a source of nitrogen and correspondingly, from qRT-PCR, the *PSY* mRNA was less abundant in nitrate-grown cells (Figure S1A and S1C). From these data we conclude that the amiRNA down-regulated the *PSY* mRNA. We confirmed this conclusion by 5'-RACE detection of *PSY* mRNA cleavage products at the amiRNA target site (Figure S1D).

The amiRNA-producing cells died in light in the presence of nitrate (Figure 1B) most likely due to silencing of *PSY* mRNA by the amiRNA and to the consequent lack of the photoprotective function of

PSY (McCarthy et al. 2004). Consistent with this interpretation the cell death was dependent on the light intensity (Figure S1B) and it did not occur in cells using ammonium rather than nitrate as nitrogen source where the amiRNA promoter is repressed (Figure 1B). We therefore used the light-induced cell death to screen for mutants in amiRNA silencing pathways.

Two independent amiRNA lines (named A4-1 and E9-3) were mutagenised by random genomic insertion of either spectinomycin or hygromycin resistance cassettes. The mutagenized cells grew well on solid medium with ammonium as nitrogen source but, unlike cultures of wild type cells expressing the amiRNA, there were some cells that grew in nitrate (Figure 1C). We hypothesised that amiRNA silencing of *PSY* had failed in these nitrate-tolerant cells due to a mutation either in the amiRNA gene, in the amiRNA biogenesis pathways or in the effector machinery of amiRNA silencing.

To further characterise forty-eight of these nitrate-tolerant lines we used northern blotting with probes for the PSY amiRNA, cre-miR1151b, cre-miR1162 and for a siRNA from a *gypsy* transposon locus (Figure 1D). Of these lines, twenty-two were depleted in the PSY amiRNA but without any effect on the endogenous sRNAs. These mutants are likely to affect the amiRNA gene and were not analysed further. In the other lines the amiRNA and endogenous sRNAs were reduced to different extents: group I mutants had reduced levels of miRNAs but not the siRNA; group II were depleted for all tested sRNAs; group III sRNAs were slightly less abundant than in wild type cells and they were heterodispersed in size; group IV sRNAs were depleted for the *gypsy* siRNA and amiRNA and had reduced levels of endogenous miRNAs (Figure 1D; Table S1). From these data we conclude that there may be separate but overlapping pathways for miRNA- and siRNA-mediated silencing. The mutant cells grew well and we further conclude that these RNA silencing pathways are not required for normal growth of the algal cells in solid or liquid media in normal laboratory conditions.

Mapping of DCL3 mutants

Because mutant strains in Group II displayed the most severe molecular phenotype, we decided to characterize them in detail. Restriction enzyme site-directed amplification (RESDA-)PCR revealed that three Group II mutations were in *DCL3*. The mutagenic inserts were in: exon 29 (mutant 51;

Figure 1D and 2A); the 3'UTR with a deletion that extended to the 5' end of its neighbour gene *Cre07.g345900* (mutant 47, Figure 1D); and exon 6 (mutant 37) (Figure S2A). The *PSY* mRNA was at wild type levels in these lines (Figure S2B) and, corresponding to the absence of the amiRNA, we could not detect the miRNA cleavage products of the *PSY* mRNA (Figure S2C).

Final confirmation of *DCL3* mutation was by complementation of mutant 51 with bacterial artificial chromosomes (BACs) (BAC A6 and BAC M20) carrying the genomic sequence corresponding to *DCL3* (*Cre07.g345900*). After transformation of mutant 51, only two independent colonies had the extra copy of *DCL3* in their genome. Importantly, these complemented lines were light sensitive when PSY amiRNA was induced with nitrate (Figure 2B) and they regained the capacity to produce endogenous miRNAs (Figure 2C). Henceforth we refer to the original lines isolated from the screen as carrying *dcl3-1* (mutant 37), *dcl3-2* (mutant 47), and *dcl3-3* (mutant 51).

C. reinhardtii DCL3 has the typical DCL domain organization except that, like the other DCLs in this alga, it lacks a PAZ domain that could be detected by primary and secondary structure prediction algorithms (Figure S3A). This protein is also exceptional amongst other DCL proteins in that it has a proline rich region (39/52 residues) on the amino terminal side of the RNase III motifs although a similar domain is also found in a related protein – Drosha. Drosha also has RNAse III motifs, and it is involved in the first steps of the animal miRNA biogenesis pathway (Figure S3A and S3B).

DCL3 and sRNA biogenesis

The northern blot analysis indicated a requirement of DCL3 for biogenesis of both siRNAs and miRNAs (Figure 1D). To extend this analysis on a genome-wide basis we sequenced sRNAs from two wild type parental lines and two *dcl3* lines (*dcl3-1* and *dcl3-3*). Consistent with previous reports (Molnar et al., 2007; Zhao et al., 2007), the sRNAs from lines expressing the amiRNA were mostly 20-to-22 nt long, with a clear peak at 21-nt that was absent in the *dcl3* mutants. As observed previously, the 21nt sRNAs had a bias towards U or A as first nucleotide (Molnár et al. 2007; Zhao et al. 2007), and those with a 5' U were clearly reduced in *dcl3* mutants (Figure 3A). The heterogeneity

of both 20 and 21 nt long small RNAs was also diminished in *dcl3* mutants, as observed in the analysis of non-redundant reads (Figure 3B).

To identify the DCL3-dependent sRNA loci we aligned libraries of sRNA sequence from wild type and *dcl3* lines to the reference genome of *C. reinhardtii*. There were 5152 sRNA loci identified in all samples of which 4313 (83.7%) were differentially expressed between the wild type parental cells and the *dcl3* mutant lines. The majority of these, 3366 (65.3%), were expressed at a higher level in the parental lines than in the mutant.

To evaluate the effect of *dcl3* loss of function on miRNA production, taking into account of a controversy about the number of miRNA genes in *C. reinhardtii* (Nozawa et al. 2012; Taylor et al. 2014), we carried out a stringent *de novo* prediction of miRNAs from all the identified sRNA loci present in both wild type- and mutant-derived samples (see Materials and Methods). This prediction indicated the presence of eighteen canonical miRNA loci in *C. reinhardtii*, denominated here "high confidence miRNAs" (Table 1). These high confidence miRNAs include seven out of the nine miRNAs identified by Taylor *et al.* (Taylor et al. 2014), as well as other previously reported/predicted miRNAs. Northern blot confirmed the production, as well as DCL3-dependency, of three out of four novel high confidence miRNAs found by our prediction tool (Table 1, Figure S4). Twenty-four additional loci specified precursor RNAs with miRNA-like features, but lacking a miRNA*, with more than one major sRNA species per arm, or with a variable 5' end. These candidate miRNA loci were assigned to "medium confidence miRNAs" (Table 1). Only sixteen out of the fifty miRNA precursors currently annotated in miRBase v.21 were identified by our stringent prediction and, in agreement with a previous analysis (Taylor et al. 2014), it is likely that the others are misannotated siRNA loci.

The miRNAs or candidate miRNAs from all class loci were less abundant in *dcl3-1* and *dcl3-3* cells than in the corresponding parental lines (Table 1, Table S2). Many (61.1%) of the high confidence miRNAs were derived from introns (9 miRNAs) or UTRs (2 miRNAs) of mRNA precursors. The medium confidence miRNA candidates were also from mRNA precursors (75%) but

they corresponded to UTRs (11 miRNAs) more than introns (7 miRNAs). The remaining miRNAs in both classes fell into a more canonical class, derived from non-coding RNAs (Table 1).

We refer to the non-miRNAs as siRNAs and we classified the genomic siRNA loci into 3 major classes corresponding to protein coding genes, transposable elements and repeat elements. We further classified transposons and repeat associated siRNAs based on the output of "repeat masker" (Table S2). All types of siRNA were predominantly dependent on DCL3, including *gypsy* siRNAs (Figure 1). However there were some protein-coding genes and non-LTR transposons (SINEX, RE, RTE) at which siRNA production was as great or greater in the *dcl3* mutants than in the wild type parents (DE dcl3>wt and NDE in Table S2). These DCL3-independent siRNAs, as well as the marginal amount of miRNAs produced in *dcl3-1* and *dcl3-3* (Table 1), were presumably generated either by DCL1 or DCL2.

Processing of intron-derived miRNAs in *Chlamydomonas*

Intron-derived (id-)miRNAs are not unique to *C. reinhardtii*: they are also found in animals. The maturation of id-miRNAs in animals referred to as miRtron (Ruby et al. 2007) is linked to intron splicing. To investigate this possibility in *C. reinhardtii*, we assembled a spectinomycin resistance gene with a miRNA-containing intron embedded in the coding sequence (*spect/intron(mi)*). The intron was from a *C. reinhardtii* gene (*Cre12.g537671*) and it contained the stem loop RNA that is the precursor of the high confidence cre-miR1157 but with the miRNA sequence modified to target the mRNA of the tryptophan synthase beta-subunit (Maa7) (Figure 4A). Silencing of *Maa7* confers resistance to 5-fluoro indole (5-FI) (Rohr et al. 2004). Control constructs either lacked an intron (*spect*) or had an intron without the miRNA stem loop (*spect/intron*) (Figure 4A).

The id-miRNA was spliced efficiently from these RNAs because the *spec/intron(mi)* construct conferred spectinomycin resistance as efficiently as the *spec* and *spec/intron* controls (Figure S5A). RT-PCR further confirmed correct splicing of the id-miRNA (Figure S5B and S5C), and a sRNA northern blot (Figure 4B) showed, as predicted, production of the mature Maa7 amiRNA. The id-miRNA was fully functional as it silenced the *Maa7* mRNA so that the *spec/intron(mi)* cells were

resistant to 5-Fl. Cells with the control constructs without the id-miRNA did not produce the amiRNA and they were fully susceptible to 5-FI (Figure 4B).

Finally, to analyse the requirement for splicing in miRNA biogenesis we generated an id-miRNA construct with a mutation in the splice donor site (Figure 4C, *spec/Δintron(mi)*). This construct conferred resistance to 5-FI but, as expected, not to spectinomycin (Figure 4D). From our results in Figure 4 and Figure S5 it is clear that the presence of the id-miRNA does not prevent the intron processing and that, unlike animal miRtrons, the intron processing is not required for miRNA biogenesis.

Differential gene expression in *dcl3* mutants

To identify mRNA targets of miRNAs we used RNA-seq of the transcriptome in *dcl3* mutant and parental lines. There were 118 annotated genes with statistically significant difference (equal or greater than 0.9 likelihood) in abundance between the *dcl3-1* and *dcl3-3* mutants and the corresponding wild type parental cells (Table S3).

The 118 DCL3-sensitive RNAs were in several classes corresponding to:

(i) non-coding RNAs with miRNA precursors (5 genes);

(ii) non-coding RNAs with siRNA precursors (64 genes);

(iii) mRNAs with miRNA precursors in the exons corresponding to the coding sequence (1 gene) and 3' UTR (8 genes);

(iv) mRNAs with siRNA precursors in the exons corresponding to the 5'UTR (5 genes), coding sequence (3 genes) and 3' UTR (21 genes);

(v) mRNAs with fold back RNA structures producing no clear siRNAs (9 genes).

The predicted and confirmed miRNA-targeted mRNAs from *C. reinhardtii* (Molnár et al. 2007; Zhao et al. 2007) were conspicuously absent from the list of differentially expressed RNAs (Table S3). These RNAs were equally abundant in the RNA-seq datasets of wild type and *dcl3* mutant lines (Figure 5A) despite the presence of the miRNA guided mRNA cleavage products only in the RNA

samples from the wild type strains (Figure 5B-C). Presumably the miRNA-directed cleavage products are present at only low abundance in these samples.

The primary effect of DCL3 on mRNA accumulation must be by direct cleavage of the mature mRNA as shown for two examples in Figure 6. These are mRNAs for which the exonic reads are more abundant in the *dcl3* mutant rather than wild type samples (Figure 6 and Table S3). The miRNA reads corresponding to the respective 3'UTRs are conversely more abundant in wild type samples (Figure 6 and Table 1). The other forty-five mRNAs accumulating at higher level in the *dcl3* mutants correspondingly were from mRNAs containing miRNA/siRNA-like stem-loop structures in their coding or non-coding exons (Table S3).

Most mRNAs with id-miRNAs, with the exception of the mRNA linked to cre-miR1154, were not affected by *dcl3* mutation (Figure S6). Based on these examples and results with the cre-miR1157 precursor (Figure 4 and Figure S5), we conclude that the DCL3 cleavage must be separate from mRNA splicing.

DISCUSSION

From our genetic analysis described here, we have identified the DCL3 protein of *C. reinhardtii* as being responsible for sRNA biogenesis and mRNA accumulation. Our findings reinforce the idea that the miRNA silencing system in this alga is distinct from that of land plants and that it may have features in common with the functional equivalent in animals. It is clear, however, from the phenotype of *dcl3* mutants that, unlike animals and land plants, miRNA silencing in *C. reinhardtii* is not required for normal growth and development. Our findings have implications for understanding the evolution and biological function of miRNA silencing in eukaryotes.

miRNA silencing in *C. reinhardtii* is not typical of higher plants

DCL3 in *C. reinhardtii* has two features that are characteristic of similar proteins in non-plant organisms. The first of these is the absence of a PAZ domain (Figure S3) as with Dicer from the human parasite *Toxoplasma gondii*. This protozoan protein, together with the three DCLs from *C.*

reinhardtii, forms a clade that is independent of both higher plant and animal DCLs (Figure 1B in Braun et al. 2010).

The PAZ domain mediates the cleavage site selection in the miRNA precursor and size specification of the miRNA (MacRae et al. 2007) and, in its absence, it is likely that other proteins carry out these functions. Perhaps the large domain replacing PAZ in *C. reinhardtii* DCL3 is the anchoring site for such accessory functions in miRNA biogenesis. The proteins encoded by uncharacterized group II mutant loci are candidates for these accessory factors (Table S1).

The second non-plant feature of DCL3 is a proline-rich domain on the amino terminal side of the two RNase III domains. There is a similar domain in an equivalent position in Drosha, the animal miRNA processor, which has an RNase III and lacks a PAZ domain (Ha and Kim 2014). These similarities prompt the hypothesis that *C. reinhardtii* DCL3 is both a Dcr and a Drosha with roles at several stages in miRNA biogenesis. The higher plant DCL1 is similarly involved in miRNA processing at early stages in addition to the final pre-miRNA cleavage (Brodersen and Voinnet 2009) but, unlike *C. reinhardtii* DCL3, it does not have any specific Drosha feature.

The miRNA genes of *C. reinhardtii*, like the DCL3 protein, also have non-plant characteristics. The most striking of these features is their overlap with protein coding genes (Table 1). This is a frequent feature of animal miRNAs whereas higher plant miRNAs are, with only few exceptions, from non-coding RNA precursors. It is estimated in animals that ~40% of the entire miRNA population are from introns (Kim et al. 2009) whereas in plants there are only three experimentally validated id-miRNAs (one and two in *A. thaliana* and *Oryza sativa*, respectively) (Rajagopalan et al. 2006; Zhu et al. 2008; Joshi et al. 2012). In one of these examples the *Arabidopsis* DCL1 strongly represses *DCL1* mRNA abundance by cleavage of an miRNA precursor in intron fourteen (Xie et al. 2003; Rajagopalan et al. 2006). In contrast, in *Chlamydomonas*, the id-miRNAs do not affect the abundance of the corresponding mRNA (Table S3) or the miRNA-induced phenotype (Figure 4) and so, even when higher plants have some id-miRNAs, there are major differences from the *Chlamydomonas* situation.

A second non-plant feature associated with the miRNA-related mechanisms of *C. reinhardtii* is with the UTR miRNAs. The mRNAs with miRNA structures in the UTR over-accumulated in the *dcl3* mutants indicating that they are targeted for degradation by DCL3 in wild type cells (Table S3). An equivalent mechanism occurs with the mammalian *FSTL1* mRNA that is destabilized by Drosha during hs-miR198 biogenesis (Sundaram et al. 2013). Similarly the *DGCR8* mRNA is destabilized by Drosha cleavage via cleavage of a hairpin-like structure at the 3'UTR although there is no miRNA produced (Han et al. 2009).

There are thirteen mRNAs in *C. reinhardtii* with miRNA in their UTRs (Table 1) of which eight accumulate at higher level in *dcl3* mutants (Table S3). In addition there are twenty-six mRNAs with siRNA precursors in their UTRs (Table S3) and nine mRNAs with hairpin structures without associated sRNAs that are up-regulated in *dcl3* (Table S3). It is likely, therefore that there are at least forty-three mRNAs in *C. reinhardtii* that may be subject to direct cleavage by DCL3. Remarkably six out of thirteen UTR miRNAs bind AGO3 (Voshall et al. 2015), one of the three AGO proteins in *C. reinhardtii*. These observations prompt us to suggest that *C. reinhardtii* DCL3, like animal Drosha, has a dual role in mRNA regulation: it is firstly a ribonuclease that controls the levels of certain mRNAs by direct cleavage and secondly it is involved in biogenesis of sRNAs that act *in trans* to influence either mRNA accumulation or translation (Ma et al. 2013; Yamasaki et al. 2013; Voshall et al. 2015).

Finally, a third non-plant feature associated with *C. reinhardtii* miRNAs concerns the complementarity requirement for miRNAs to produce an effective down-regulation of their targets. Effective miRNA silencing in higher plants depends on near complete complementarity of the miRNA and its target (Liu et al. 2014) whereas, in *C. reinhardtii*, pairing in the miRNA seed region is sufficient to induce down-regulation (Yamasaki et al. 2013).

Evolution of miRNA silencing in *C. reinhardtii*

Animal and plant miRNA pathways are very different and it is likely that they evolved separately from an ancestral RNA silencing pathway with Dicer proteins and small RNAs with 5' phosphate and

3’ hydroxyl groups that bind to AGO proteins (Ghildiyal and Zamore 2009; Axtell et al. 2011). The algal/*Chlamydomonas* miRNA pathway is also distinct from that of higher plants, as discussed above, and we can envision either of two evolutionary scenarios to explain those differences. The first of these is that animal, higher plant and algal miRNA pathways all evolved independently of each other. A second scenario is that an animal-like miRNA pathway evolved early and persisted in lower plant lineages including the green algae and *C. reinhardtii*, although it was not retained in higher plants.

Our data are consistent with the second scenario because *C. reinhardtii* and animal miRNA pathways share the presence of a Drosha-like structure (absence of PAZ and presence of P-rich domain) of the miRNA processing enzyme (Figure S3), Drosha-like dual function exerted by the miRNA processing enzyme (Figure 6 and Table S3), and miRNA association with introns or exons of RNA coding sequences (Table 1). In addition, as mentioned above, the animal and *C. reinhardtii* miRNA systems depend only on seed region complementarity (Yamasaki et al. 2014) and they both employ VIG and TSN1 (Voshall et al. 2015; Ibrahim 2009).

At present there are insufficient data to resolve these two alternative scenarios although the further characterisation of additional class I –IV mutants (Table S1) may shed more light on the evolutionary origin of miRNAs in *C. reinhardtii*.

The role of sRNAs in *C. reinhardtii*

To explain the absence of physiological phenotype in our *dcl3* mutants in normal laboratory conditions as described here and in a description of another unrelated RNA silencing mutant of *Chlamydomonas* (Voshall et al. 2015) we propose that DCL3 has a role at certain stages of the life cycle or under conditions that have not yet been tested. A role under starvation of sulphate and/or phosphate is possible because these conditions affect sRNA profiles in *Chlamydomonas* (Shu and Hu 2012; Zheng et al. 2015). The DCL3-dependent silencing might also act redundantly with other silencing systems as indicated by the loss of transposon silencing in *C. reinhardtii* that was dependent on loss of function at both DCL1 and of a histone methyltransferase (Casas-Mollano et al. 2008). The availability of DCL3 mutants will now allow us to test these possibilities. We cannot, however, rule

out the possibility that at least some of the *C. reinhardtii* sRNAs have a silencing-independent role or that they are some form of junk RNA.

METHODS

Strain, culture conditions and transformation

The *C. reinhardtii* cell-wall deficient strain CC-1883 (*cw15, NIA, NIT2, mt*$^{-}$) was used in this study as wild type background. It was obtained from the *Chlamydomonas* Resource Center (University of Minnesota) and grown in either solid or liquid 2-amino-2-(hydroxymethyl)-1,3-propanediol (TRIS)-acetate-phosphate (TAP) media (Harris 2009) at 25 °C under continuous illumination. When indicated, cells were grown in nitrate TAP (TAP medium in which ammonium was replaced by the equivalent amount of nitrate).

For transformation, the indicated DNA cassettes were excise from their backbones, and around 100 ng of purified fragments were used for each transformation experiment. Transformations of mid-log-phase cells were done by electroporation following a previously described method (Shimogawara et al. 1998) in a Gene Pulser Xcell™ apparatus (Bio-Rad) with exponential electric pulses (2250 kV/cm, 10 µF). After recovery, cells were plated on solid media in the presence of starch.

DNA oligonucleotides

DNA sequence of primers used in this study are listed in Table S4.

Plasmids

The nitrate-inducible amiRNA construct (ni-amiRNA) was generated from pMS539 (Schmollinger et al. 2010) by subcloning a *Xba*I/*Dra*I excised fragment that contains the Nit1 promoter/5'UTR, amiRNA precursor and terminator into *Xba*I/*Sma*I digested pSI103-1 (a derivative of pSI103, Sizova et al. 2001). Unlike the original pMS539, the resulting plasmid confers resistance to paromomycin once integrated into the *C. reinhardtii* genome.

The amiRNA that targets *PSY* (*Cre02.g095092*) mRNA was designed using the Web MicroRNA Designer (http://wmd3.weigelworld.org/). The 21-nt amiRNA 5'-UGAUUUUGGAAGCGUUCGGCC-3' was introduced in ni-amiRNA as a 90-nt double-stranded DNA (obtained by *in vitro* annealing of amiFor-PSY and amiRev-PSY primers) in its unique *Spe*I restriction site, following a previously described method (Molnár et al. 2009), to generate the ni-amiRNA-PSY.

The intron-derived cre-miR1157 precursor that lacks of the cre-miR1157 stem-loop was amplified by PCR from ni-amiRNA with primers miR1157-Prec-For and miR1157-Prec-Rev, which carry tails in order to reconstitute the whole intron 22 from *Cre12.g537671* and add *Pml*I and *Pvu*II restriction sites at the 5' and 3' ends of the PCR product, respectively. This PCR product was cloned into pGEM-T Easy (Promega) to create pGEMT-miR1157. The gene splicing via overlap extension method (Horton et al. 1989) was used to generate the *Spect/intron*, a plasmid based on pALM32 (Meslet-Cladière and Vallon 2011) that carries the whole intron-derived cre-miR1157 (without the stem loop precursor) in the middle of the *aadA* gene. A mix of three different DNA fragments was used as template for the overlapping PCR: (i) a PCR product obtained by amplification from pALM32 using the primers RBSC2_Pro-For and Spect+intron1157-Rev; (ii) a PCR product obtained by amplification from pALM32 using the primers Spect+intron1157-For and RBSC2_3'UTR-Rev; and (iii) a *Pml*I/*Pvu*II digested fragment from pGEMT-miR1157. The resulting PCR fragment was digested with *Kpn*I and cloned into *Sma*I/*Kpn*I digested pALM32 to generate the *Spect/intron* plasmid. *Spect/intron(mi)* was generated by cloning an amiRNA (5'-UAUGUACACAAUGCACUUCAG-3'), which targets the tryptophan synthase beta-subunit mRNA, into the *Spect/intron* plasmid by following the procedure described above. Site-directed mutagenesis of the splicing donor site in *Spect/intron(mi)* was carried out by two PCR steps, as previously described (Herlitze and Koenen 1990). The first round PCRs were done by using *Spect/intron(mi)* as template plus primer pair HSP70-For and Intron_Donor-Mut-Rev primers, or primers Intron_Donor-Mut-For and SpeI-Rev. These two PCR products were then used as template for the second round PCR with primers HSP70-For and SpeI-Rev. The resulting PCR product was digested with *Aat*II/*Spe*I

and cloned by triple ligation with *Aat*II/*Hind*III and *Spe*I/*Hind*III digested fragments from *Spect/intron(mi)* to generate *Spect/*Δ*intron(mi)*.

BAC clones 29A6 (A6) and 29M20 (M20) carrying the *C. reinhardtii* DCL3 genomic sequence were identified in a BAC library generated by Paul Lefebvre (University of Minnesota) by using the JGI v4 browser (http://genome.jgi-psf.org/Chlre4/Chlre4.info.html). The whole library, named CRCCBa, was obtained from Clemson University Genomics Institute and the indicated clones were isolated from *E. coli* glycerol stocks by using the QIAGEN Large-Construct Kit (Qiagen) following the manufacturer's instructions.

Plasmids pSI103-1 (J. Moy, M. LaVoie and C. Silflow; unpublished results), pHyg3 (Berthold et al. 2002), and pALM32 (Meslet-Cladière and Vallon 2011) were obtained from the *Chlamydomonas* Resource Center (University of Minnesota).

Mutant Screen and mapping of mutagen integration sites

Two independent transgenic lines (here called A4-1 and E9-3 parental lines) carrying a functional ni-amiRNA cassette were grown on liquid TAP until mid-log-phase (this medium carries ammonium as the only nitrogen source, which represses the Nit1 promoter). Random insertional mutants were obtained by transformation of A4-1 and E9-3 with the corresponding resistance cassettes from pALM32 and pHyg3, respectively, following the transformation protocol described above. Mutant lines potentially affected in the miRNA silencing pathway were observed at 5-7 days after plating the cells in solid amiRNA induction media (TAP medium in which the ammonium was replaced for an equivalent amount of nitrate) at high light intensity (200 µmol photons $m^{-2}sec^{-1}$). Insertions were mapped in the *C. reinhardtii* genome by RESDA-PCR as previously described (González-Ballester et al. 2005). Primer pairs annealing across the insertion sites were used for easy genotyping of dcl3 mutant lines by direct PCR, from a tiny amount of cells, by using Phire Plant Direct PCR Kit (Thermo Scientific) according to the manufacturer's instruction.

RNA extraction and analyses

RNA isolation and small RNA detection by northern blot were carried out as previously described (Molnár et al. 2007). A detailed protocol can be found at http://www.plantsci.cam.ac.uk/research/davidbaulcombe/methods/downloads/smallrna.pdf/view. DNA primers corresponding to the reverse complementary sequence of the indicated miRNAs (amiRPSY-det, miR1151b-det, miR1157-det, miR1162-det, siRgypsy-det, miR_Cre07.g341100-det, miR_Cre07.g344260-det, miR_Cre14.g623850-det and miR_Cre16.g670000-det in Table S4) were radiolabelled with γ^{32}P-ATP by the action of polynucleotide kinase and used to probe membranes with immobilized RNA samples. Radioactive signals were further detected with a phosphorimager.

The accumulation level of *PSY* mRNA was estimated by qRT-PCR from 5 µg of DNA-free RNA. Briefly, RT was primed with random hexamers and SuperScript III (Invitrogen) following manufacturer's guidelines. The PCR amplification step was carried out with primers PSY-qPCR-For and PSY-qPCR-Rev in the presence of the dsDNA-specific dye SYBR Green (Sigma) and monitored with a Chromo4 qPCR machine (Bio-Rad). The *RACK1* gene (*Cre06.g278222*) was used as internal control for normalization. The delta-delta Ct method was used to calculate the differences in mRNA abundance.

RT-PCR was used to confirm splicing of the artificially generated, intron-derived, miRNA precursor. To do that, RT reaction was carried out as described above, whereas a normal PCR amplification step with primers Spect-For and Spect-Rev, which flank both sides of the intron, was done using the RT reaction as template.

5′ RNA ligase-mediated RACE was done as described (Llave et al. 2002) with the GeneRacer kit (Invitrogen). First PCR round was done with distal primers (PSY-Rev, OMT2-Rev and CPLD52-Rev) while nested primers were used for the second round PCRs (PSY_nested-Rev, OMT2_nested-Rev, CPLD52_nested-Rev). The final PCR fragments were gel purified using MinElute gel extraction kit (Qiagen), and cloned into pCR®II vector (Invitrogen). Positive clones were further analysed by DNA sequencing to map exact miRNA cleavage sites.

Preparation of RNA libraries

Prior to prepare sRNA libraries, samples carrying 10 µg of total RNA were subjected to the FDF-PAGE method as previously described (Harris et al. 2015). The sRNA libraries were further prepared according to the TruSeq small RNA cloning protocol (Illumina), and run in an Illumina HiSeq 2000 (BGI Hong Kong).

Libraries for RNA-seq were prepared from poly-A RNAs, which were purified from 50 µg of total RNA by using the MicroPoly(A)Purist Kit (Ambion), following the manufacturer's instructions. Poly-A RNA was used as starting material for the ScriptSeq™ v2 RNA-seq Library Preparation Kit (Illumina). Libraries were prepared following the manufacturer's protocol and run in an Illumina HiSeq 2000 (BGI Hong Kong).

Analysis of sRNA High-throughput sequencing data

Illumina sRNA libraries were pre-processed using the ADDAPTS pipeline and tracking system (http://www.plantsci.cam.ac.uk/bioinformatics/addapts). After 3' adaptor removal, all sequences less than 15nt in length are discarded and the remaining sequences are aligned against *C. reinhardtii* genome v5.0 using PatMaN (Prüfer et al. 2008). Only sequences with at least one perfect match are included. The initial sequencing data for each library, as well as the number of reads obtained after each step, are indicated in Table S5. For the definition of sRNA producing loci, segmentSeq_2.2.1 (Hardcastle et al. 2012), available as part of Bioconductor, was used. This package takes the density of matches of sRNAs to the genome to determine regions corresponding to sRNA producing transcripts, taking into account replicate data. Segments with a higher than 0.9 posterior probability of being loci were used. Loci were subjected to differential expression analysis using baySeq 2.2.0 (Hardcastle and Kelly 2010). This package uses the negative binomial distribution for the count data produced by high-throughput sequencing and estimates its parameters using empirical Bayes, with the number of iterations determined by the parameter 'sample size'. Models for different patterns of differential expression (including no differential expression) among the samples are specified and the model with the highest posterior probability is used. The library scaling factor (surrogates for library size) has to be specified for each sample, and they were calculated by using the previously described

quantile normalization (Bullard et al. 2010). This method sum all counts in each sample for which the value below the qth quantile of non-zero counts for that particular sample. Only those loci with a likelihood ≥ 0.9 of being differently expressed in the specified model were considered as differentially expressed loci.

A python (v2.7.9) script was developed to count the number of overlaps between genomic annotations (Phytozome v5.5), repeat masker annotations (Phytozome v10.3), inverted repeats, tandem repeats, and miRNA precursors (these three last features were predicted as explained below) with the sets of differentially and non-differentially expressed loci. Inverted repeats and tandem repeats were predicted by Inverted Repeat Finder v3.0.7 and Tandem Repeat Finder v4.0.7b, respectively (Warburton et al. 2004; Benson 1999).

MiRNA prediction

The identification of miRNA precursors was performed by a multi-step process, which firstly uses a combination of three different miRNA prediction algorithms: miRDP, miRDeep2 (with minimum score of 5) and miRCat (Yang and Li 2011; Mackowiak 2011; Stocks et al. 2012). These results were then combined to remove duplicate predictions, precursors with mature miRNAs with sizes outside 20-to-22nt, and/or precursors with less than 100 sRNA reads. Finally, the last automated step was performed by removing those predicted miRNA precursors that did not overlap with those sRNA loci that had been previously identified by segmentSeq (see above). The resulting precursors were manually curated for the presence of miRNA* and defined miRNA stacks in an attempt to follow the standards of high confidence recommended by miRBase (Kozomara and Griffiths-Jones 2014). The number of identified miRNA precursors at each stage of the multi-step process is shown in Table S6. Detailed information about predicted miRNA precursors (exact location in the genome, as well as nucleotide sequences of the corresponding mature miRNAs and miRNAs*) is shown in Table S7.

Analysis of RNA-seq High-throughput sequencing data

RNA-seq libraries were first analysed with fastqc v0.11.2 for quality control (http://www.bioinformatics.babraham.ac.uk/projects/fastqc/). Trimmomatic 0.32 (Bolger et al. 2014) was then used for adaptor removal and trimming of bases with a quality score lower than 20. Reads shorter than 40nt were discarded and the remaining reads were subsequently aligned to rRNA, ncRNA, cpDNA and mtDNA from *C. reinhardtii* using Bowtie 2 (Langmead and Salzberg 2012). Positive matches were discarded. Finally the remaining reads were aligned with Bowtie 2 against the *C. reinhardtii* transcriptome (Phytozome v5.5). The initial sequencing data for each library, as well as the number of reads obtained after each filtering step, are indicated in Table S5. Quantification of transcript abundance was performed using express 1.5.1 (Roberts and Pachter 2013). The est_counts and eff_length from express were then passed as input to baySeq (Hardcastle and Kelly 2010) for the differential expression analysis. Transcripts for which a likelihood ≥ 0.9 in the specified model were considered as differentially expressed.

DATA ACCESS

Small RNA-seq and RNA-seq datasets generated during this study have been submitted to ArrayExpress database (EMBL-EBI; https://www.ebi.ac.uk/arrayexpress/) under accession numbers E-MTAB-3851 and E-MTAB-3852, respectively.

ACKNOWLEDGMENTS

We thank James Barlow for technical assistance and media preparation, Michael Schroda and Stefan Schmollinger for providing pMS539, Olivier Vallon for his useful advice about BACs as well as DNA sequencing data. We thank Witold Filipowicz and Ian Henderson for critical reading of the manuscript. Work in the Baulcombe laboratory is supported by the Balzan Prize award and the ERC Advanced Investigator Grant ERC-2013-AdG 340642 TRIBE. AAV was supported by a Marie-Curie fellowship (PIEF-GA-2010-276037). BYC was supported by an EMBL long-term postdoctoral fellowship and a Sir Henry Wellcome Fellowship (096082). DCB is the Royal Society Edward Penley Abraham Research Professor.

AAV and DCB designed the research. AAV performed most of the experiments. BACMS analyzed high-throughput sequencing data. SH maps the mutation in the *dcl3-3* allele. AB, AM and BYC designed and carried out experiments leading to the identification of a mutant affecting miRNA and siRNA pathways. AAV and DCB wrote the manuscript.

FIGURE LEGENDS

Figure 1. Screening and isolation of mutants affected in miRNA-mediated RNA silencing. (A) Schematic representation of the artificial miRNA construct used to transform the wild type strain. Transgenic lines carrying this cassette were further screened by random insertional mutagenesis (P_{RBSC2}: RuBisCO small subunit (RBSC)2 promoter; Paromomycin^{R}: *Streptomyces rimosus* AphVIII coding gene; T_1: RBSC2 transcription terminator; P_{Nit1}: Nitrate reductase promoter; PSY amiRNA: modified version of cre-miR1157 that carries a miRNA against the phytoene synthase; T_2: RLP12 transcription terminator). (B) Selective cell death of transgenic lines expressing the PSY amiRNA in the presence of nitrate, but not ammonium, as the sole nitrogen source. Transgenic lines carrying the empty amiRNA vector (EV) were used as control. (C) Growth in high light conditions of mutagenized (Spect^{R}) and non-mutagenized (-) reporter lines (PSY $_{amiRNA}$) in solid media containing either nitrate or ammonium as sole nitrogen source. Transgenic lines carrying the empty amiRNA vector (EV) and further transformed with the spectinomycin resistant cassette were used as control. (D) Detection by northern blot of diverse small RNAs in total RNA samples from the indicated mutants and controls. These mutants were obtained by random insertional mutagenesis of either spectinomycin or hygromycin resistant cassettes. The mutants were grouped (I-IV, Table S1) based on the molecular phenotype. The two displayed mutants belonging to the group II corresponds to the characterized mutant 47 (*dcl3-2)* and mutant 51 (*dcl3-3)*.

Figure 2. Mapping and complementation of group II mutant #51 (A) Location of the mutagenic hygromycin resistant cassette in the Mutant #51. (B) Phenotype of the indicated parental line and both complemented and non-complemented lines (biological triplicates) in the presence of either nitrate or

ammonium under high light conditions. (C) Detection by northern blot of the indicated miRNAs in total RNA samples from the *C. reinhardtii* strains analyzed in B.

Figure 3. Effect of *dcl3* mutation on sRNA of *C. reinhardtii* small RNA population. (A) Size-distribution histograms of sRNAs from the parental line A4-1 and its derivative *dcl3-1* mutant, expressed as the number of counted reads of a given size per million (CPM) of reads matching the *C. reinhardtii* genome. The percentage of 21-nt sRNAs with their 5′ nucleotide identities is also shown. (B) Size-distribution histograms of non-redundant sRNAs from the parental line A4-1 and its derivative *dcl3-1* mutant, expressed as CPM of reads matching the *C. reinhardtii* genome. Two additional replicates per sample, as well as three replicates from E9-3 parental and *dcl3-3* lines, showed the same result.

Figure 4. The cre-miR1157 is an intron-derived miRNA. (A) Schematic representation of constructs carrying the cre-miR1157 intron inserted into the spectinomycin resistance gene coding sequence. The cre-miR1157 intron was modified to either lack the miRNA stem-loop or carry an artificial miRNA against Maa7 in *spect/intron* and *spect/intron(mi)* plasmids, respectively (P: Hybrid RBSC2/HSP70A promoter; Spectinomycin^{R}: recoded *Escherichia coli*-derived aadA coding gene; T: RBSC2 transcription terminator; SpeI: unique cleavage site for *Spe*I restriction enzyme; Maa7 amiRNA: modified version of cre-miR1157 that carries a miRNA against Maa7). (B) Top panel: growth of the indicated transgenic lines in solid media carrying spectinomycin with/without 5-Fluorindole (5-Fl). Bottom panel: Detection by northern blot of the artificial miRNA against Maa7 in total RNA samples from the indicated lines (three independent lines per construct). (C) Schematic representation of constructs used to test the requirement of splicing for the expression of id-miRNA. The GT x AT point mutations in the exon/intron junction are indicated. These plasmids also carry the Paromomycin^{R} cassette (equivalent to the cassette showed in Figure 1A) to allow the primary selection of transgenic lines in paromomycin. (D) Growth of lines transformed with the indicated plasmids in solid media containing either paromomycin (test for plasmid integration), spectinomycin (test for splicing events) or 5-Fl (test for amiRNA production).

Figure 5. The effect of miRNA on mRNA accumulation. (A) Steady-state accumulation levels of previously reported miRNA targets (Molnar et al., 2007; Zhao et al., 2007) assessed as the number of normalized reads (Y-axis) in RNA-seq data. Error bars for three independent samples are shown. The target genes with their corresponding miRNA are indicated. These miRNAs were predicted as either high confidence miRNAs (cre-miR1162, cre-miR1151a/b) or medium confidence miRNA (miR-C82) (see Table 1), with the exception of cre-miR909 that is a hairpin-derived siRNA also depleted in the *dcl3* mutant background. (B) 5'RACE to test the specific cleavage of *CPLD52* (*Cre13.g608000*) mediated by cre-miR1162. The asterisk indicates an unspecific PCR product. The PCR products were sequenced and the right hand panel shows the 5' terminus of these cleavage products aligned to the 5' to 3' mRNA sequence and the 3' to 5' miRNA. G:U base pairs are indicated by a circle (C) 5'RACE to test the specific cleavage of *OMT2* (*Cre17.g713200*) mediated by the miR-C82 (Zhao et al., 2007) with the 5' terminus of these cleavage products aligned to the 5' to 3' mRNA sequence and the 3' to 5' miRNA as in B.

Figure 6. The effect of DCL3 on mRNAs with miRNA hairpin-like structures in the 3'UTR. *Cre16.g694950* (serine/threonine kinase) (A) and *Cre24.g755697* (aminoglycoside 3'-phosphotransferase) (B) have the respective cre-miR1169 and cre-miR1172 precursors in their 3'UTR. The figure shows a schematic representation of both genes with their exons (blue boxes) and introns (blue dotted lines) at the bottom of each panel. Green (A4-1 parental line) and red (*dcl3-1*) hills represent sRNA and mRNA read counts. Both panels show the results for one replicate of A4-1 parental line and its *dcl3-1* derivative knock out mutant. Over-accumulation (X-fold) of the indicated mRNA in *dcl3-1* regarding the A4-1 parental line is indicated. Two additional samples from this parental and mutant line combination, as well as a biological triplicate from E9-3 parental and dcl3-3 derivative lines showed the same trend in both miRNA and mRNA accumulation (Table 1 and Table S3).

REFERENCES

Axtell MJ, Westholm JO, Lai EC. 2011. Vive la différence: biogenesis and evolution of microRNAs

in plants and animals. *Genome Biol* **12**: 221.

Bartel DP. 2009. MicroRNAs: target recognition and regulatory functions. *Cell* **136**: 215–233.

Baulcombe D. 2004. RNA silencing in plants. *Nature* **431**: 356–363.

Baumgarten S, Bayer T, Aranda M, Liew YJ, Carr A, Micklem G, Voolstra CR. 2013. Integrating microRNA and mRNA expression profiling in Symbiodinium microadriaticum, a dinoflagellate symbiont of reef-building corals. *BMC Genomics* **14**: 704.

Benson G. 1999. Tandem repeats finder: a program to analyze DNA sequences. *Nucleic Acids Res* **27**: 573–580.

Berthold P, Schmitt R, Mages W. 2002. An engineered Streptomyces hygroscopicus aph 7" gene mediates dominant resistance against hygromycin B in Chlamydomonas reinhardtii. *Protist* **153**: 401–412.

Bolger AM, Lohse M, Usadel B. 2014. Trimmomatic: a flexible trimmer for Illumina sequence data. *Bioinformatics* **30**: 2114–2120.

Braun L, Cannella D, Ortet P, Barakat M, Sautel CF, Kieffer S, Garin J, Bastien O, Voinnet O, Hakimi MA. 2010. A complex small RNA repertoire is generated by a plant/fungal-like machinery and effected by a metazoan-like argonaute in the single-cell human parasite Toxoplasma gondii. *PLoS Pathog* **6**: e1000920.

Brodersen P, Voinnet O. 2009. Target Recognition and Mode of Action. **10**: 141–148.

Carthew RW, Sontheimer EJ. 2009. Origins and Mechanisms of miRNAs and siRNAs. *Cell* **136**: 642–655.

Casas-Mollano JA, Rohr J, Kim EJ, Balassa E, Van Dijk K, Cerutti H. 2008. Diversification of the core RNA interference machinery in Chlamydomonas reinhardtii and the role of DCL1 in transposon silencing. *Genetics* **179**: 69–81.

Castel SE, Martienssen RA. 2013. RNA interference in the nucleus: roles for small RNAs in transcription, epigenetics and beyond. *Nat Rev Genet* **14**: 100–112.

Chen XS, Collins LJ, Biggs PJ, Penny D. 2009. High throughput genome-wide survey of small RNAs from the parasitic protists Giardia intestinalis and Trichomonas vaginalis. *Genome Biol Evol* **1**:

165–175.

Ghildiyal M, Zamore PD. 2009. Small silencing RNAs: an expanding universe. *Nat Rev Genet* **10**: 94–108.

González-Ballester D, De Montaigu A, Galván A, Fernández E. 2005. Restriction enzyme site-directed amplification PCR: A tool to identify regions flanking a marker DNA. *Anal Biochem* **340**: 330–335.

Ha M, Kim VN. 2014. Regulation of microRNA biogenesis. *Nat Rev Mol Cell Biol* **15**: 509–524.

Han J, Pedersen JS, Kwon SC, Belair CD, Kim Y-K, Yeom K-H, Yang W-Y, Haussler D, Blelloch R, Kim VN. 2009. Posttranscriptional crossregulation between Drosha and DGCR8. *Cell* **136**: 75–84.

Hardcastle TJ, Kelly KA. 2010. baySeq: empirical Bayesian methods for identifying differential expression in sequence count data. *BMC Bioinformatics* **11**: 422.

Hardcastle TJ, Kelly KA, Baulcombe DC. 2012. Identifying small interfering RNA loci from high-throughput sequencing data. *Bioinformatics* **28**: 457–463.

Harris CJ, Molnar A, Muller SY, Baulcombe DC. 2015. FDF-PAGE: a powerful technique revealing previously undetected small RNAs sequestered by complementary transcripts. *Nucleic Acids Res* 1–9.

Harris EH. 2009. *The Chlamydomonas Sourcebook: Introduction to Chlamydomonas and Its Laboratory Use*. Academic Press, New York.

Herlitze S, Koenen M. 1990. A general and rapid mutagenesis method using polymerase chain reaction. *Gene* **91**: 143–147.

Horton RM, Hunt HD, Ho SN, Pullen JK, Pease LR. 1989. Engineering hybrid genes without the use of restriction enzymes: gene splicing by overlap extension. *Gene* **77**: 61–68.

Huang PJ, Lin WC, Chen SC, Lin YH, Sun CH, Lyu PC, Tang P. 2012. Identification of putative miRNAs from the deep-branching unicellular flagellates. *Genomics* **99**: 101–107.

Ibrahim F. 2009. *Molecular characterization of RNA interference components in Chlamydomonas: A novel nucleotidyltransferase (MUT68) and a Vasa intronic gene homolog (MUT70)*. The

University of Nebraska, Lincoln.

Iwasaki YW, Siomi MC, Siomi H. 2015. PIWI-Interacting RNA: Its Biogenesis and Functions. *Annu Rev Biochem* **84**: 405–433.

Joshi PK, Gupta D, Nandal UK, Khan Y, Mukherjee SK, Sanan-Mishra N. 2012. Identification of mirtrons in rice using MirtronPred: A tool for predicting plant mirtrons. *Genomics* **99**: 370–375.

Kim VN, Han J, Siomi MC. 2009. Biogenesis of small RNAs in animals. *Nat Rev Mol Cell Biol* **10**: 126–139.

Langmead B, Salzberg SL. 2012. Fast gapped-read alignment with Bowtie 2. *Nat Methods* **9**: 357–359.

Llave C, Xie Z, Kasschau KD, Carrington JC. 2002. Cleavage of Scarecrow-like mRNA targets directed by a class of Arabidopsis miRNA. *Science* **297**: 2053–2056.

Mackowiak SD. 2011. Identification of novel and known miRNAs in deep-sequencing data with miRDeep2. *Curr Protoc Bioinformatics* **12**: Unit 12.10.

MacRae IJ, Zhou K, Doudna J a. 2007. Structural determinants of RNA recognition and cleavage by Dicer. *Nat Struct Mol Biol* **14**: 934–940.

Mallick B, Ghosh Z, Chakrabarti J. 2008. MicroRNA switches in Trypanosoma brucei. *Biochem Biophys Res Commun* **372**: 459–463.

Mar-Aguilar F, Trevino V, Salinas-Hernández JE, Taméz-Guerrero MM, Barrón-González MP, Morales-Rubio E, Treviño-Neávez J, Verduzco-Martínez JA, Morales-Vallarta MR, Reséndez-Pérez D. 2013. Identification and characterization of microRNAs from Entamoeba histolytica HM1-IMSS. *PLoS One* **8**: e68202.

McCarthy SS, Kobayashi MC, Niyogi KK. 2004. White mutants of Chlamydomonas reinhardtii are defective in phytoene synthase. *Genetics* **168**: 1249–1257.

Meister G. 2013. Argonaute proteins: functional insights and emerging roles. *Nat Rev Genet* **14**: 447–459.

Merchant SS, Prochnik SE, Vallon O, Harris EH, Karpowicz SJ, Witman GB, Terry A, Salamov A, Fritz-Laylin LK, Maréchal-Drouard L, et al. 2007. The Chlamydomonas genome reveals the

evolution of key animal and plant functions. *Science* **318**: 245–250.

Meslet-Cladière L, Vallon O. 2011. Novel shuttle markers for nuclear transformation of the green alga Chlamydomonas reinhardtii. *Eukaryot Cell* **10**: 1670–1678.

Molnár A, Bassett A, Thuenemann E, Schwach F, Karkare S, Ossowski S, Weigel D, Baulcombe D. 2009. Highly specific gene silencing by artificial microRNAs in the unicellular alga Chlamydomonas reinhardtii. *Plant J* **58**: 165–174.

Molnár A, Schwach F, Studholme DJ, Thuenemann EC, Baulcombe DC. 2007. miRNAs control gene expression in the single-cell alga Chlamydomonas reinhardtii. *Nature* **447**: 1126–1129.

Nozawa M, Miura S, Nei M. 2012. Origins and evolution of microRNA genes in plant species. *Genome Biol Evol* **4**: 230–239.

Prüfer K, Stenzel U, Dannemann M, Green RE, Lachmann M, Kelso J. 2008. PatMaN: rapid alignment of short sequences to large databases. *Bioinformatics* **24**: 1530–1531.

Rajagopalan R, Vaucheret H, Trejo J, Bartel DP. 2006. A diverse and evolutionarily fluid set of microRNAs in Arabidopsis thaliana. *Genes Dev* **20**: 3407–3425.

Roberts A, Pachter L. 2013. Streaming fragment assignment for real-time analysis of sequencing experiments. *Nat Methods* **10**: 71–73.

Rohr J, Sarkar N, Balenger S, Jeong BR, Cerutti H. 2004. Tandem inverted repeat system for selection of effective transgenic RNAi strains in Chlamydomonas. *Plant J* **40**: 611–621.

Ruby JG, Jan CH, Bartel DP. 2007. Intronic microRNA precursors that bypass Drosha processing. *Nature* **448**: 83–86.

Saraiya AA, Wang CC. 2008. snoRNA, a novel precursor of microRNA in Giardia lamblia. *PLoS Pathog* **4**: e1000224.

Schmollinger S, Strenkert D, Schroda M. 2010. An inducible artificial microRNA system for Chlamydomonas reinhardtii confirms a key role for heat shock factor 1 in regulating thermotolerance. *Curr Genet* **56**: 383–389.

Shimogawara K, Fujiwara S, Grossman A, Usuda H. 1998. High-efficiency transformation of Chlamydomonas reinhardtii by electroporation. *Genetics* **148**: 1821–1828.

Shu L, Hu Z. 2012. Characterization and differential expression of microRNAs elicited by sulfur deprivation in Chlamydomonas reinhardtii. *BMC Genomics* **13**: 108.

Sizova I, Fuhrmann M, Hegemann P. 2001. A Streptomyces rimosus aphVIII gene coding for a new type phosphotransferase provides stable antibiotic resistance to Chlamydomonas reinhardtii. *Gene* **277**: 221–229.

Stocks MB, Moxon S, Mapleson D, Woolfenden HC, Mohorianu I, Folkes L, Schwach F, Dalmay T, Moulton V. 2012. The UEA sRNA workbench: a suite of tools for analysing and visualizing next generation sequencing microRNA and small RNA datasets. *Bioinformatics* **28**: 2059–2061.

Sundaram GM, Common JE a, Gopal FE, Srikanta S, Lakshman K, Lunny DP, Lim TC, Tanavde V, Lane EB, Sampath P. 2013. "See-saw" expression of microRNA-198 and FSTL1 from a single transcript in wound healing. *Nature* **495**: 103–106.

Taylor RS, Tarver JE, Hiscock SJ, Donoghue PCJ. 2014. Evolutionary history of plant microRNAs. *Trends Plant Sci* **19**: 175–182.

Voshall A, Kim E-J, Ma X, Moriyama EN, Cerutti H. 2015. Identification of AGO3-Associated miRNAs and Computational Prediction of Their Targets in the Green Alga Chlamydomonas reinhardtii. *Genetics* **200**: 105–121.

Warburton PE, Giordano J, Cheung F, Gelfand Y, Benson G. 2004. Inverted repeat structure of the human genome: the X-chromosome contains a preponderance of large, highly homologous inverted repeats that contain testes genes. *Genome Res* **14**: 1861–1869.

Yang X, Li L. 2011. miRDeep-P: a computational tool for analyzing the microRNA transcriptome in plants. *Bioinformatics* **27**: 2614–2615.

Yoon HS, Hackett JD, Ciniglia C, Pinto G, Bhattacharya D. 2004. A Molecular Timeline for the Origin of Photosynthetic Eukaryotes. *Mol Biol Evol* **21**: 809–818.

Zhao T, Li G, Mi S, Li S, Hannon GJ, Wang XJ, Qi Y. 2007. A complex system of small RNAs in the unicellular green alga Chlamydomonas reinhardtii. *Genes Dev* **21**: 1191–1203.

Zheng Y, Wang Y, Wu J, Ding B, Fei Z. 2015. A dynamic evolutionary and functional landscape of plant phased small interfering RNAs. *BMC Biol* **13**: 1–15.

Zhu QH, Spriggs A, Matthew L, Fan L, Kennedy G, Gubler F, Helliwell C. 2008. A diverse set of microRNAs and microRNA-like small RNAs in developing rice grains. *Genome Res* **18**: 1456–1465.

Table 1: Stringent *de novo* prediction of miRNA precursors in *C. reinhardtii* .

							Quantification****			
Group	**Chromosome**	**Start**	**Gene ID**	**Location**	**Protein size (aa)****	**Conserved domains/protein ID**	**Previously described*****	**A4-1**	**dcl3-1 (A4-1)**	**E9-3**	**dcl3-3 (E9-3)**
High confidence	chromosome_2	739310	*Cre02.g078500*			Predicted non-coding RNA	cre-miR911	1211	6	1261	6
	chromosome_4	3100624	*Cre04.g225700*	intron	263	MED8	cre-miR1153	5729	21	6202	16
	chromosome_4	3820425	*Cre04.g229776*			Predicted non-coding RNA	cre-miR1155	35	0	21	0
	chromosome_5	3227666	*Cre05.g239950*	exon	1053	Predicted protein	miR-C89	6554	23	5013	25
	chromosome_6	3067368	*Cre06.g274550*	intron	1035	Protein Kinase	cre-miR1162	8384	45	10812	27
	chromosome_6	6776108	*Cre06.g294776*			Predicted non-coding RNA	miR-cluster20399	27189	192	22255	129
	chromosome_6	7063792	*Cre06.g296983*	intron	750	Ubiquitin-activating Enzyme E1	cre-miR1152	651	1	470	2
	chromosome_7	2371057	*Cre07.g328400*	intron	482	RNA-binding Protein	cre-miR1151a	10862	31	6052	33
	chromosome_7	2372822	*Cre07.g328400*	intron	482	RNA-binding Protein	cre-miR1151b	6891	19	4542	19
	chromosome_7	4386252	*Cre07.g341100**			Predicted non-coding RNA		3264	27	1926	19
	chromosome_7	4631481	*Cre07.g344260**			Predicted non-coding RNA		399	12	232	11
	chromosome_7	5926395	*Cre07.g354150*	intron	621	MFT22	miR-C59	95	0	66	0
	chromosome_8	121858	*Cre08.g358535*			Predicted non-coding RNA	miR-cluster22587	6137	55	5484	64
	chromosome_12	6402226	*Cre12.g537671*	intron	3661	SNF2-Chromodomain	cre-miR1157	3089	8	2683	5
	chromosome_14	2347075	*Cre14.g623850*	3'UTR	703	Protein Kinase		3770	16	4148	15
	chromosome_14	3218783	*Cre14.g629200*	intron	522	FAP98	cre-miR910	11688	54	7694	46
	chromosome_16	4056196	*Cre16.g670000*			Predicted non-coding RNA		4604	38	5194	22
	chromosome_17	6144120	*Cre17.g741601*	3'UTR	528	Predicted protein	miR-cluster12551	802	31	750	28
Medium confidence	chromosome_1	3724965	*Cre01.g023913*			Predicted non-coding RNA		1139	29	969	33
	chromosome_1	5106349	*Cre01.g035500*	intron	1191	Phosphatidylinositol-3-kinase	miR-C82	700	2	586	0
	chromosome_1	7070552	*Cre01.g051050**			Predicted non-coding RNA		404	18	273	2
	chromosome_2	2217872	*Cre02.g089850*	3'UTR	471	Histone chaperone Rttp106-like		611	10	459	8
	chromosome_2	8349161	*Cre02.g141426*			Predicted non-coding RNA		141	14	133	13
	chromosome_2	9101133	*Cre02.g143327*	intron	541	Predicted protein	miR-cluster14705	1176	195	59	1
	chromosome_2	9129508	*Cre02.g143427*	3'UTR	252	Trypsin-like peptidase domain	miR-cluster14712	1192	94	904	6
	chromosome_2	9173306	*Cre02.g143527*	3'UTR	289	Trypsin-like peptidase domain	miR-cluster14719	489	262	315	6
	chromosome_3	6573899	*Cre03.g195950*	3'UTR	763	GAG-POL-Related-Retrotransposon	miR-n062	169	0	237	0
	chromosome_4	457811	*Cre04.g217925*	intron	554	KELCH Repeat Domain	cre-miR1144b	312	15	129	1
	chromosome_4	3694793	*Cre04.g229050*	intron	745	Inositol polyphosphate kinase 1	cre-miR1154	423	3	446	1
	chromosome_5	1790702	*Cre05.g242301*	3'UTR	313	Predicted protein	cre-miR913	2521	1284	1657	87
	chromosome_7	5632709	*Cre07.g352150*	5'UTR	226	Protein Kinase		113	2	156	3
	chromosome_8	126807	*Cre08.g358537*	intron	483	Predicted protein - DUF3431		315	1	380	0
	chromosome_9	6365928	*Cre09.g406983*	intron	278	Cobalamin synthesis protein	cre-miR912	5964	43	4450	36
	chromosome_10	3399870	*Cre10.g444300*			Predicted non-coding RNA	cre-miR9897	62594	246	42741	228
	chromosome_10	6282484	*Cre10.g465000*	3'UTR	566	Protein Kinase	miR-cluster3318	69	1	85	1
	chromosome_13	2001067	*Cre13.g576700*	3'UTR	603	Predicted protein	miR-cluster7085	17026	310	9869	184
	chromosome_13	2127530	intergenic			Predicted non-coding RNA		723	23	347	14
	chromosome_13	3152367	*Cre13.g585175/200*	3'UTR	335	APC1-like	miR-C112	1060	48	908	3
	chromosome_16	185088	*Cre16.g694950*	3'UTR	410	Protein Kinase	cre-miR1169	2544	17	4771	18
	chromosome_16	828236	*Cre16.g647602*	intron	1676	SNF2 family N-terminal domain		223	19	176	16
	chromosome_17	5149811	*Cre17.g735375*			Predicted non-coding RNA		1025	221	960	369
	scaffold_24	82186	*Cre24.g755697*	3'UTR	730	Protein Kinase	cre-miR1172	2158	8	2325	6

* Overlap with an annotated gene but in reverse orientation.

** Sizes in amino acids of proteins that are produced from the indicated coding and putative coding genes.

*** Previously described miRNAs are identified here with their original names: cre-miRX (miRBASE), miR-CX (Zhao et al., 2007), miR-nX (Shu and Hu, 2012), miR-clusterX (Voshall et al., 2015), where X is the number of a given miF

**** Average of normalized reads from 3 independent libraries that aligns with the miRNA precursor. Normalization was done by segmentSeq_2.2.1 (see Materials and Methods for additional information).

Additional information about predicted miRNAs and miRNA precursors can be found in Table S7.

RNA.

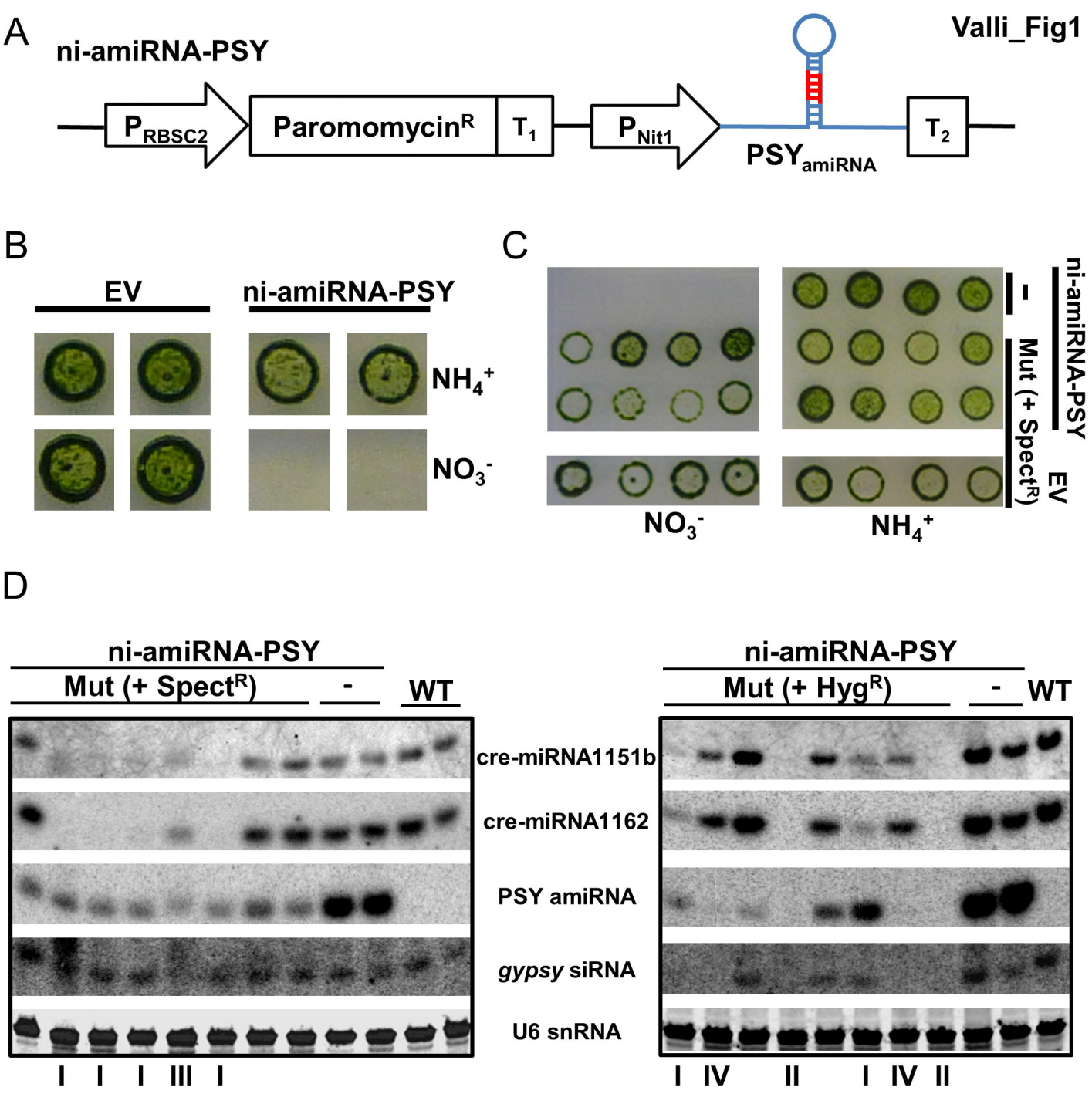
A
ni-amiRNA-PSY
Valli_Fig1
P RBSC2
Paromomycin R
T 1
P Nit1
PSY amiRNA
T 2
B
EV
ni-amiRNA-PSY
NH4+
NO3-
C
ni-amiRNA-PSY
-
Mut (+ SpectR)
EV
NO3-
NH4+
D
ni-amiRNA-PSY
Mut (+ SpectR)
-
WT
ni-amiRNA-PSY
Mut (+ HygR)
-
WT
cre-miRNA1151b
cre-miRNA1162
PSY amiRNA
gypsy siRNA
U6 snRNA
I I I III I
I IV II I IV II

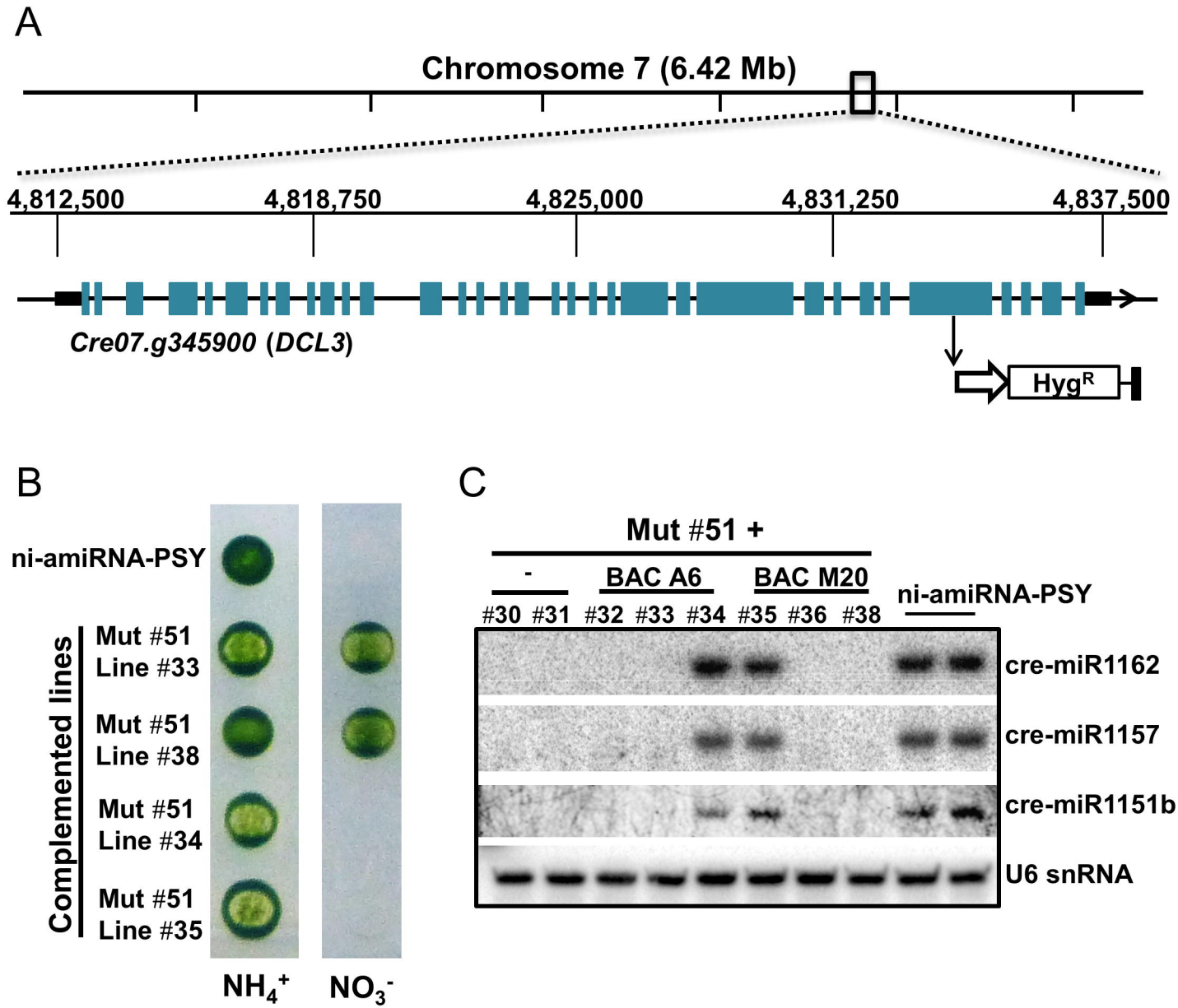
A
Chromosome 7 (6.42 Mb)
4,812,500
4,818,750
4,825,000
4,831,250
4,837,500
Cre07.g345900 (DCL3)
Hyg^R
B
ni-amiRNA-PSY
Complemented lines
Mut #51 Line #33
Mut #51 Line #38
Mut #51 Line #34
Mut #51 Line #35
NH4+
NO3-
C
Mut #51 +
-
BAC A6
BAC M20
ni-amiRNA-PSY
#30 #31 #32 #33 #34 #35 #36 #38
cre-miR1162
cre-miR1157
cre-miR1151b
U6 snRNA

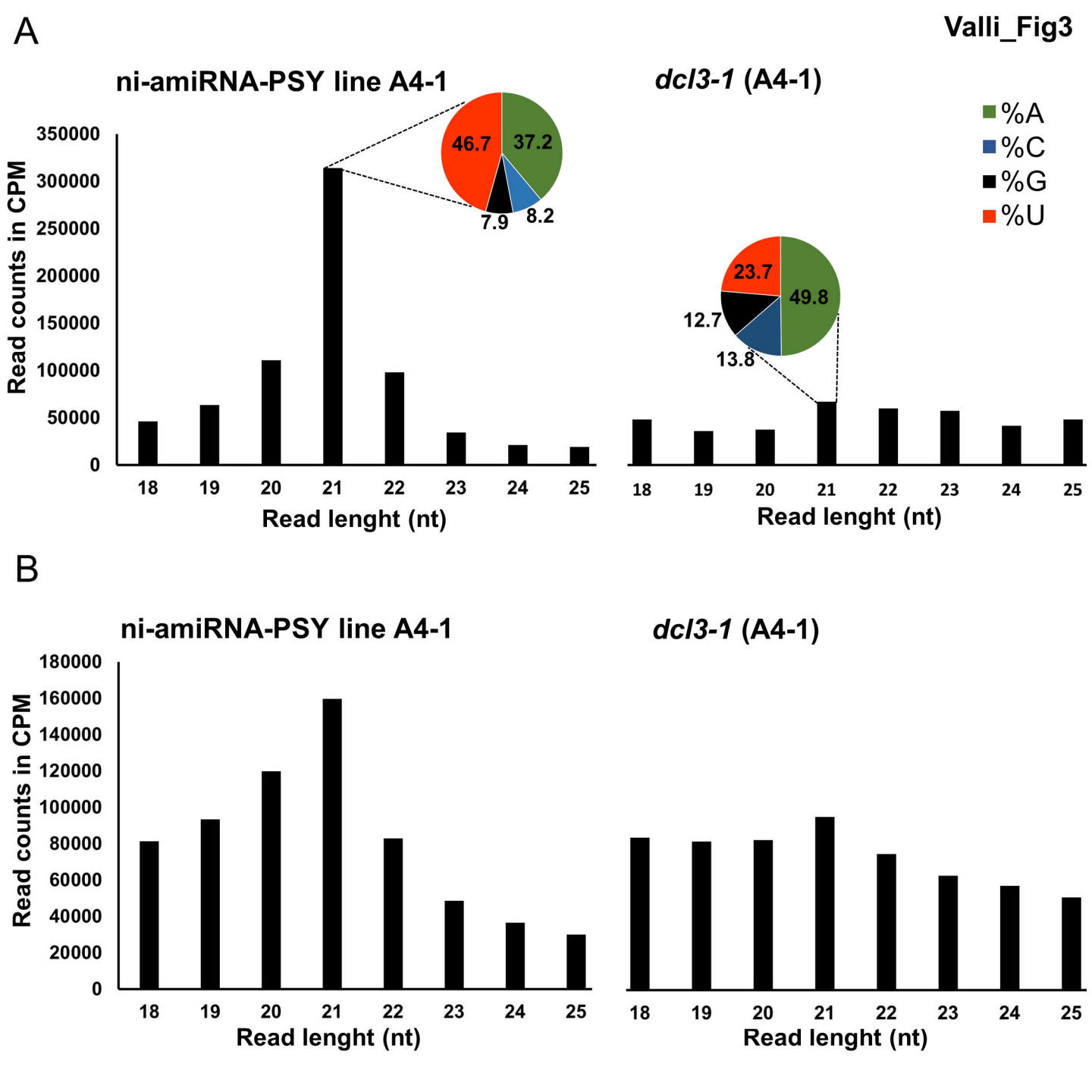
A
ni-amiRNA-PSY line A4-1
dcl3-1 (A4-1)
%A
%C
%G
%U
46.7
37.2
7.9
8.2
23.7
49.8
12.7
13.8
Read counts in CPM
350000
300000
250000
200000
150000
100000
50000
0
18
19
20
21
22
23
24
25
Read lenght (nt)
B
ni-amiRNA-PSY line A4-1
dcl3-1 (A4-1)
180000
160000
140000
120000
100000
80000
60000
40000
20000
0
Read counts in CPM
Read lenght (nt)

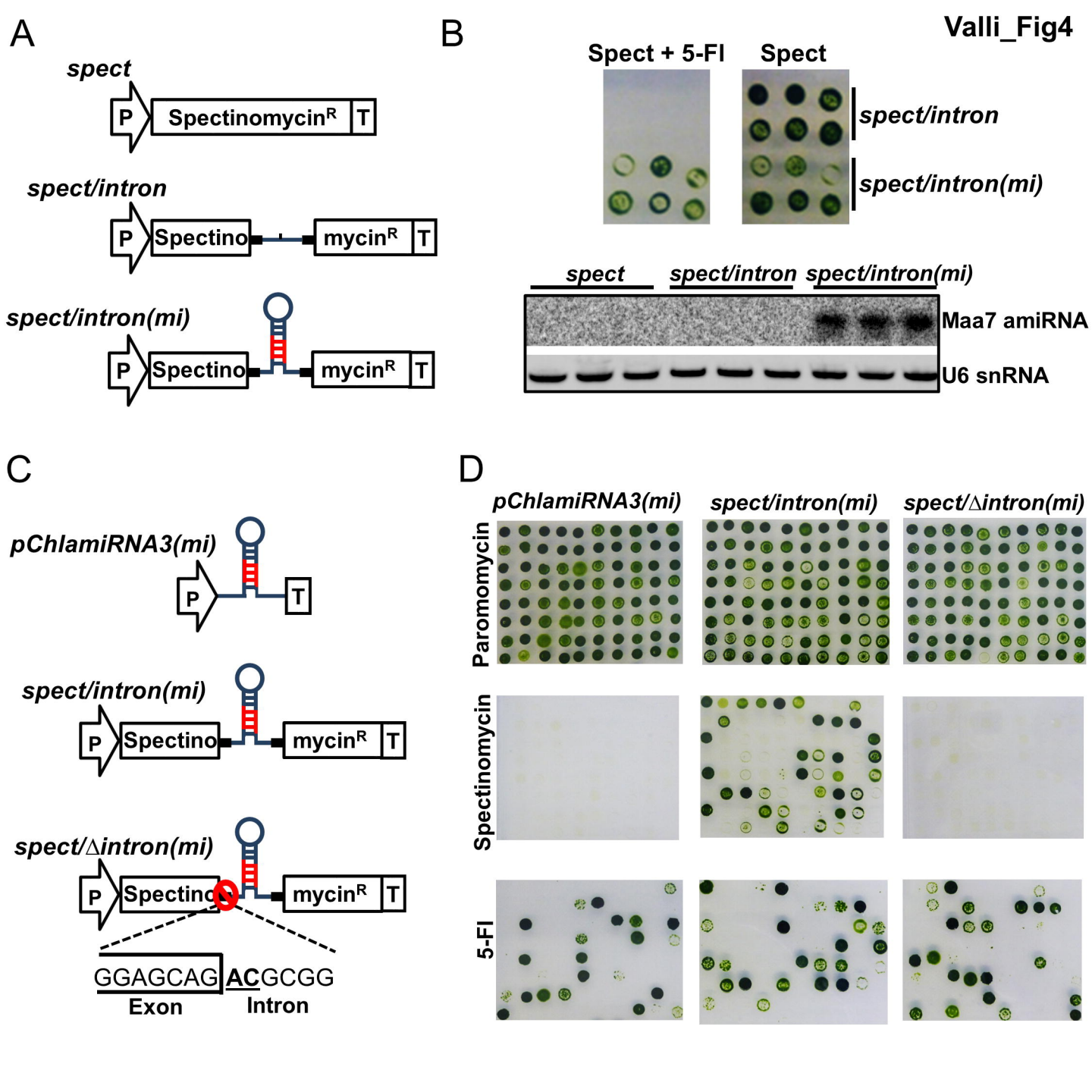
Valli_Fig4
A
spect
P
SpectinomycinR
T
spect/intron
Spectino
mycinR
spect/intron(mi)
B
Spect + 5-FI
Spect
spect/intron
spect/intron(mi)
spect
spect/intron
spect/intron(mi)
Maa7 amiRNA
U6 snRNA
C
pChlamiRNA3(mi)
spect/intron(mi)
spect/Δintron(mi)
GGAGCAG
ACGCGG
Exon
Intron
D
pChlamiRNA3(mi)
spect/intron(mi)
spect/Δintron(mi)
Paromomycin
Spectinomycin
5-FI

A

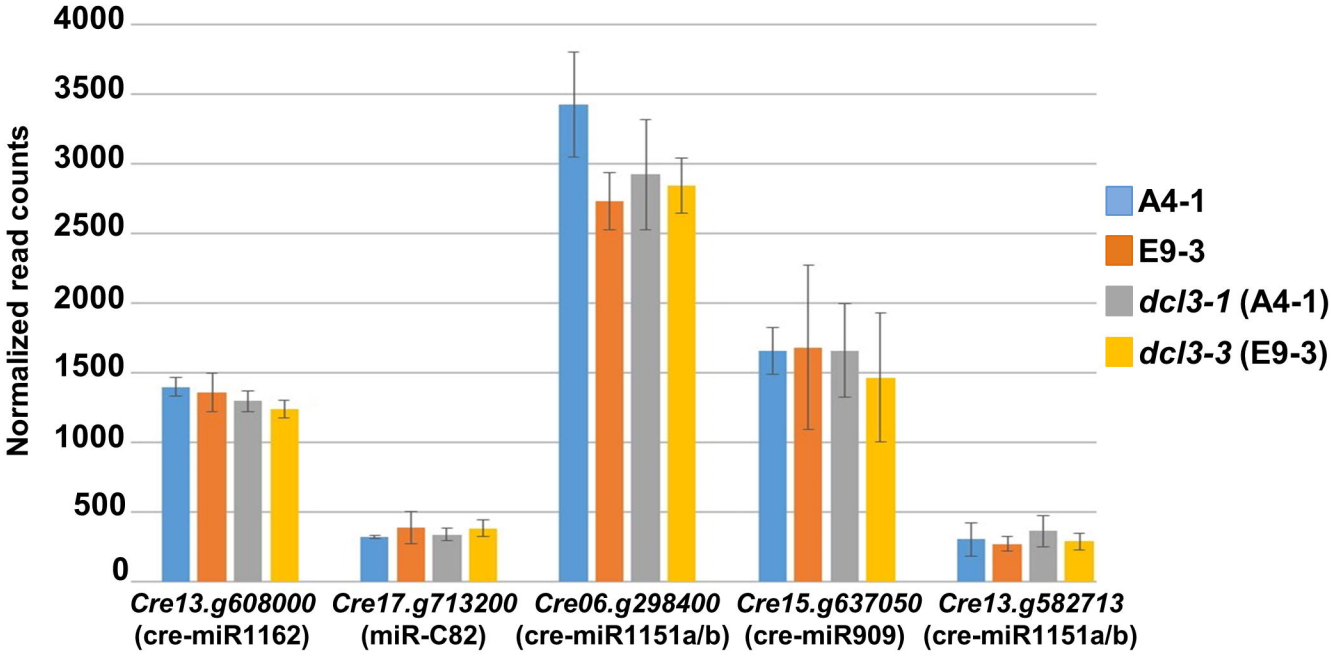
Normalized read counts
4000
3500
3000
2500
2000
1500
1000
500
0
A4-1
E9-3
dcl3-1 (A4-1)
dcl3-3 (E9-3)
Cre13.g608000 (cre-miR1162)
Cre17.g713200 (miR-C82)
Cre06.g298400 (cre-miR1151a/b)
Cre15.g637050 (cre-miR909)
Cre13.g582713 (cre-miR1151a/b)

B

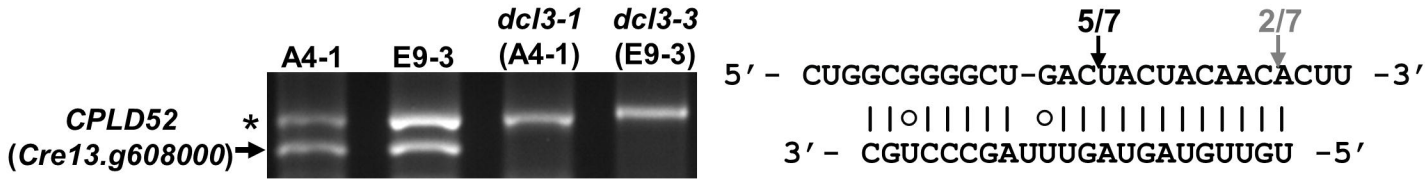
A4-1
E9-3
dcl3-1 (A4-1)
dcl3-3 (E9-3)
CPLD52 (Cre13.g608000)
*
5/7
2/7
5′- CUGGCGGGGCU-GACUACUACAACACUU -3′
3′- CGUCCCGAUUUGAUGAUGUUGU -5′

C

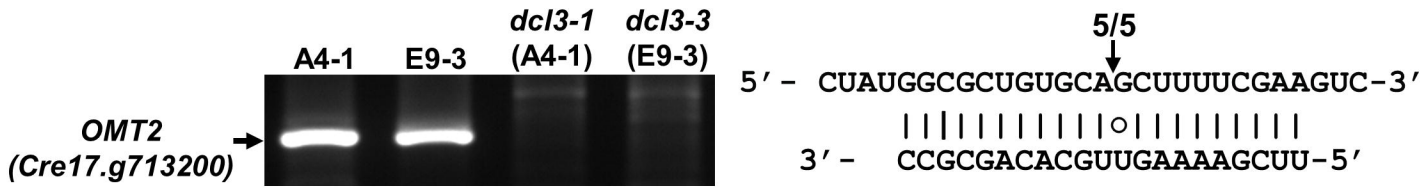
A4-1
E9-3
dcl3-1 (A4-1)
dcl3-3 (E9-3)
OMT2 (Cre17.g713200)
5/5
5′- CUAUGGCGCUGUGCAGCUUUUCGAAGUC-3′
3′- CCGCGACACGUUGAAAAGCUU-5′

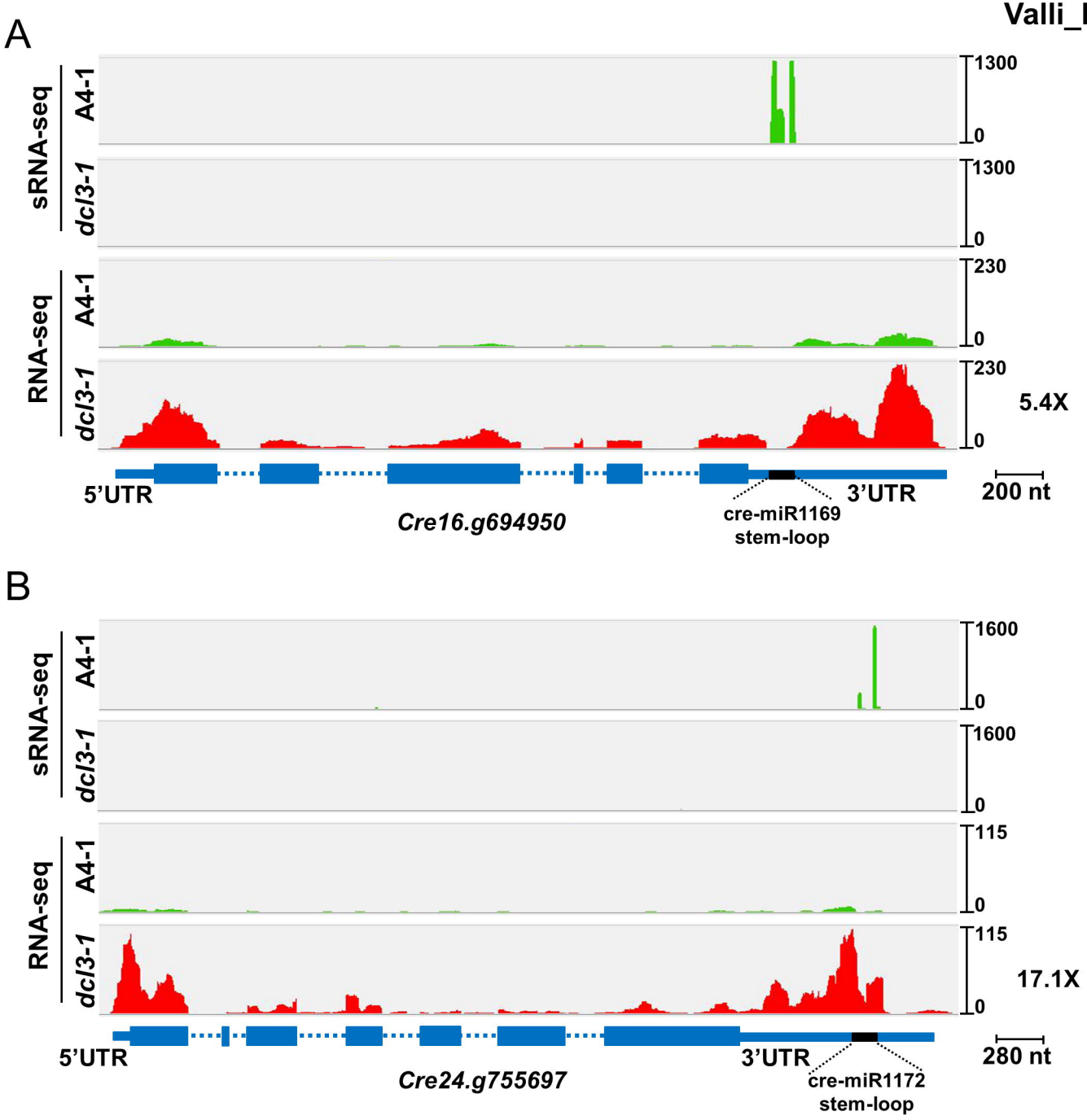
A
sRNA-seq
A4-1
dcl3-1
RNA-seq
A4-1
dcl3-1
1300
0
1300
0
230
0
230
0
5.4X
5'UTR
3'UTR
200 nt
Cre16.g694950
cre-miR1169
stem-loop
B
sRNA-seq
A4-1
dcl3-1
RNA-seq
A4-1
dcl3-1
1600
0
1600
0
115
0
115
0
17.1X
5'UTR
3'UTR
280 nt
Cre24.g755697
cre-miR1172
stem-loop